Article

Fluorescent Magnetic Nanocrystals by Sequential Addition of Reagents in a One-Pot Reaction: A Simple Preparation for Multifunctional Nanostructures

Jinhao Gao, Bei Zhang, Yuan Gao, Yue Pan, Xixiang Zhang, and Bing Xu

J. Am. Chem. Soc., **2007**, 129 (39), 11928-11935• DOI: 10.1021/ja0731017 • Publication Date (Web): 08 September 2007

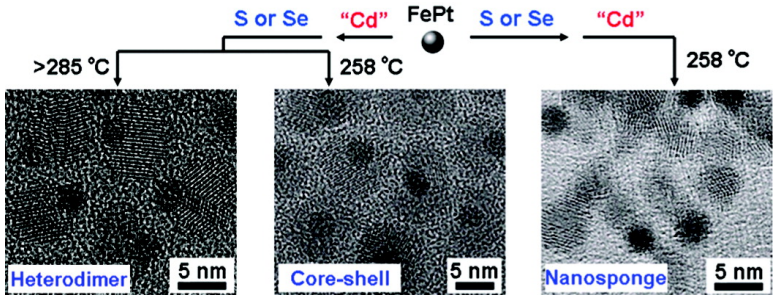

More About This Article

Additional resources and features associated with this article are available within the HTML version:

- Supporting Information
- Links to the 9 articles that cite this article, as of the time of this article download
- Access to high resolution figures
- Links to articles and content related to this article
- Copyright permission to reproduce figures and/or text from this article

View the Full Text HTML

J|A|C|S
ARTICLES
Published on Web 09/08/2007

Fluorescent Magnetic Nanocrystals by Sequential Addition of Reagents in a One-Pot Reaction: A Simple Preparation for Multifunctional Nanostructures

Jinhao Gao,[†] Bei Zhang,[‡,§] Yuan Gao,[‡] Yue Pan,[‡] Xixiang Zhang,[‡,§] and Bing Xu*[,†,‡]

Contribution from the Department of Chemistry, Graduate Program of Nano Science and Technology, and Department of Physics, The Hong Kong University of Science and Technology, Clear Water Bay, Hong Kong, China

Received May 3, 2007; E-mail: chbingxu@ust.hk

Abstract: Core−shell nanostructures consisting of FePt magnetic nanoparticles as the core and semiconducting chalcogenides as the shell were synthesized by a series of reactions in a one-pot procedure. Adding $Cd(acac)_2$ as the cadmium precursor to a reaction mixture containing FePt nanoparticles afforded FePt@CdO core−shell intermediates. The subsequent addition of chalcogens yielded FePt@CdX core−shell nanocrystals (where X was S or Se). The reverse sequence of addition, i.e., adding X before Cd, resulted in spongelike nanostructures because the chalcogens readily formed nanowires in the solution. Transmission electron microscopy, energy-dispersive X-ray spectrometry, selected area electron diffraction, fluorescence spectroscopy, and SQUID were used to characterize the nanostructures. These core−shell nanostructures displayed superparamagnetism at room temperature and exhibited fluorescence with quantum yields of 2.3−9.7%. The flexibility in the sequence of addition of reagents, combined with the compatibility of the lattices of the different materials, provides a powerful yet convenient strategy for generating sophisticated, multifunctional nanostructures.

1. Introduction

In this study set we out to synthesize fluorescent magnetic nanoparticles with a core−shell nanostructure of FePt@CdX (X = S or Se) through the sequential addition of reagents in a one-pot procedure. Nanomaterials with novel structures promise applications in many fields such as superconducting materials, biological sensors, and carriers of drug delivery.[1] The design and fabrication of sophisticated, multifunctional nanostructures has recently been attracting increased research effort, especially for biological applications.[2] Among the well-established nanomaterials, both quantum dots (QDs) and magnetic nanoparticles have found notable and successful applications in biology and biomedicine. While the former are receiving increased acceptance as fluorescent probes for visualizing biological processes in vitro and in vivo,[3,4] the latter have served as magnetic resonance imaging (MRI) agents for the diagnosis of many diseases, including cancers.[5]

Many recent studies have demonstrated the potential of quantum dots as biological probes in vitro and in vivo. For example, Nie and co-workers demonstrated the application of bioconjugates of quantum dots for ultrasensitive and multiplex biological detection and imaging.[6] Bawendi and co-workers

[†] Department of Chemistry.
[‡] Graduate Program of Nano Science and Technology.
[§] Department of Physics.

(1) (a) Murray, C. B.; Kagan, C. R.; Bawendi, M. G. *Science* **1995**, *270*, 1335. (b) Bruchez, M.; Moronne, M.; Gin, P.; Weiss, S.; Alivisatos, A. P. *Science* **1998**, *281*, 2013. (c) Milliron, D. J.; Hughes, S. M.; Cui, Y.; Manna, L.; Li, J. B.; Wang, L. W.; Alivisatos, A. P. *Nature* **2004**, *430*, 190. (d) Sun, Y. G.; Xia, Y. N. *Science* **2002**, *298*, 2176. (e) Gudiksen, M. S.; Lauhon, L. J.; Wang, J.; Smith, D. C.; Lieber, C. M. *Nature* **2002**, *415*, 617. (f) Rosi, N. L.; Giljohann, D. A.; Thaxton, C. S.; Lytton-Jean, A. K. R.; Han, M. S.; Mirkin, C. A. *Science* **2006**, *312*, 1027. (g) Nazzal, A. Y.; Qu, L. H.; Peng, X. G.; Xiao, M. *Nano Lett.* **2003**, *3*, 819. (h) Sirbuly, D. J.; Law, M.; Pauzauskie, P.; Yan, H. Q.; Maslov, A. V.; Knutsen, K.; Ning, C. Z.; Saykally, R. J.; Yang, P. D. *Proc. Natl. Acad. Sci. U.S.A.* **2005**, *102*, 7800. (i) Gao, J. H.; Liang, G. L.; Zhang, B.; Kuang, Y.; Zhang, X. X.; Xu, B. *J. Am. Chem. Soc.* **2007**, *129*, 1428. (j) Sirbuly, D. J.; Tao, A.; Law, M.; Fan, R.; Yang, P. D. *Adv. Mater.* **2007**, *19*, 61.

(2) (a) Hong, L.; Jiang, S.; Granick, S. *Langmuir* **2006**, *22*, 9495. (b) Nie, Z. H.; Li, W.; Seo, M.; Xu, S. Q.; Kumacheva, E. *J. Am. Chem. Soc.* **2006**, *128*, 9408. (c) Yang, J.; Elim, H. I.; Zhang, Q. B.; Lee, J. Y.; Ji, W. *J. Am. Chem. Soc.* **2006**, *128*, 11921. (d) Taguchi, M.; Yagi, I.; Nakagawa, M.; Iyoda, T.; Einaga, Y. *J. Am. Chem. Soc.* **2006**, *128*, 10978. (e) Choi, S. H.; Kim, E. G.; Hyeon, T. *J. Am. Chem. Soc.* **2006**, *128*, 2520. (f) Jun, Y. W.; Choi, J. S.; Cheon, J. *Angew. Chem., Int. Ed.* **2006**, *45*, 3414. (g) Teranishi, T. *Small* **2006**, *2*, 596. (h) Gao, J. H.; Zhang, B.; Zhang, X. X.; Xu, B. *Angew. Chem., Int. Ed.* **2006**, *45*, 1220. (i) Yin, Y.; Alivisatos, A. P. *Nature* **2005**, *437*, 664. (j) Yi, D. K.; Selvan, S. T.; Lee, S. S.; Papaefthymiou, G. C.; Kundaliya, D.; Ying, J. Y. *J. Am. Chem. Soc.* **2005**, *127*, 4990. (k) Selvan, S. T.; Patra, P. K.; Ang, C. Y.; Ying, J. Y. *Angew. Chem., Int. Ed.* **2007**, *46*, 2448.

(3) (a) Medintz, I. L.; Uyeda, H. T.; Goldman, E. R.; Mattoussi, H. *Nat. Mater.* **2005**, *4*, 435. (b) Cui, Y.; Wei, Q. Q.; Park, H. K.; Lieber, C. M. *Science* **2001**, *293*, 1289. (c) Stroh, M.; Zimmer, J. P.; Duda, D. G.; Levchenko, T. S.; Cohen, K. S.; Brown, E. B.; Scadden, D. T.; Torchilin, V. P.; Bawendi, M. G.; Fukumura, D.; Jain, R. K. *Nat. Med.* **2005**, *11*, 678. (d) Mattoussi, H.; Mauro, J. M.; Goldman, E. R.; Anderson, G. P.; Sundar, V. C.; Mikulec, F. V.; Bawendi, M. G. *J. Am. Chem. Soc.* **2000**, *122*, 12142. (e) Zhang, Y.; So, M. K.; Loening, A. M.; Yao, H. Q.; Gambhir, S. S.; Rao, J. H. *Angew. Chem., Int. Ed.* **2006**, *45*, 4936.

(4) Zimmer, J. P.; Kim, S. W.; Ohnishi, S.; Tanaka, E.; Frangioni, J. V.; Bawendi, M. G. *J. Am. Chem. Soc.* **2006**, *128*, 2526.

(5) Pankhurst, Q. A.; Connolly, J.; Jones, S. K.; Dobson, J. *J. Phys. D: Appl. Phys.* **2003**, *36*, R167.

(6) (a) Chan, W. C. W.; Maxwell, D. J.; Gao, X. H.; Bailey, R. E.; Han, M. Y.; Nie, S. M. *Curr. Opin. Biotechnol.* **2002**, *13*, 40. (b) Chan, W. C. W.; Nie, S. M. *Science* **1998**, *281*, 2016. (c) Gao, X. H.; Cui, Y. Y.; Levenson, R. M.; Chung, L. W. K.; Nie, S. M. *Nat. Biotechnol.* **2004**, *22*, 969. (d) Gao, X. H.; Yang, L. L.; Petros, J. A.; Marshal, F. F.; Simons, J. W.; Nie, S. M. *Curr. Opin. Biotechnol.* **2005**, *16*, 63.

10.1021/ja0731017 CCC: $37.00

reported the creation of InAs/ZnSe core−shell quantum dots which fluoresced at near-infrared wavelengths and demonstrated their applications for in vivo imaging.[4,7] Mattoussi et al. used quantum dot−peptide conjugates to monitor proteolytic activity by fluorescence resonance energy transfer (FRET).[8] Kotov et al. applied a layer-by-layer approach to forming quantum dot-based stable ultrathin films with regular periodicities[9] and used the self-assembly of CdTe nanocrystals to mimic protein folding.[10] Rao and co-workers reported an elegant approach which used bioluminescence to "turn on" the fluorescence of quantum dots in an intracellular molecular imaging process.[11] Moreover, quantum dots with narrow and tunable fluorescence properties can be covalently linked to oligonucleotides and used as probes for detecting DNA with desired sequences.[12] The most prominent biomedical application of magnetic nanoparticles has been as contrast agents in MRI, where they are gaining clinical acceptance.[13] Recently, techniques and procedures for producing monodispersed magnetic nanoparticles or nanorods (for example, FePt, CoPt, FePd, Fe_3O_4, and γ-Fe_2O_3) are close to being perfected.[14,15] Several groups have explored the applications of such magnetic nanomaterials in MRI and as magnetic carriers for drug delivery, pathogen detection, or protein separation.[16] For example, Weissleder and co-workers developed a cell-labeling approach to track the distribution and differentiation of progenitor and stem cells using Tat peptides linked with magnetic nanoparticles.[17] Moreover, they developed a novel, biocompatible, and physiologically inert iron oxide nanoparticle for in vivo MRI tracking of injected cells at near-single-cell resolution.[18]

Such exciting and successful applications have inspired the fabrication of nanostructures that exhibit both fluorescence and magnetism, including FePt−CdS heterodimer nanoparticles,[19] γ-Fe_2O_3/MS (M = Zn, Cd, or Hg) heterojunctions,[20] FePt−ZnS nanosponges,[21] Fe_2O_3 bead−CdSe/ZnS quantum dot nanocomposites,[22] and Co@CdSe core−shell nanocomposites.[23] At the same time, other multicomponent and multifunctional nanostructures have also emerged, for example, $CoPt_3$−Au heterodimer nanocrystals,[24] Au−Fe_3O_4 dumbbell-like bifunctional nanoparticles,[25] CdSe−Au heterostructures,[26] Fe_3O_4−Ag and FePt−Ag heterodimer nanocrystals,[27] and other binary or ternary hybrid nanostructures.[28] Despite the successful synthesis of these sophisticated nanostructures, there has been little reported effort to systematically explore the sequence of the addition of the reagents and its influence on the formation of the nanostructures.

In this study we aimed to develop a convenient means for controlling the morphology of multifunctional nanostructures by altering the sequence of addition of their reagents. Using as-prepared FePt nanoparticles as seeds, two types of fluorescent magnetic nanostructures were generated through a one-pot synthesis procedure. As shown in Scheme 1, the addition of $Cd(acac)_2$ as a cadmium precursor promoted the formation of FePt@CdO core−shell intermediate nanostructures, and then the subsequent addition of a chalcogen yielded FePt@CdX core−shell nanocrystals, where X denotes S or Se (this will be termed route 1). The reverse sequence of precursor addition yielded nanosponges of FePt−CdX (X = S or Se). Apparently, the addition of chalcogens allowed the formation of nanowires of chalcogens in hot solution (about 120 °C), which served to connect FePt nanoparticles; the subsequent addition of $Cd(acac)_2$ gave FePt−CdX nanosponges (route 2).

Variables controlling the formation of these nanostructures, reaction conditions and the ratios of precursors, were varied systematically, and the structures of the resulting products were observed. For example, use of a higher boiling point solvent in the route 1 synthesis was observed to result in the formation of FePt−CdX heterodimer nanocrystals. These appear to be the

(7) Kim, S. W.; Zimmer, J. P.; Ohnishi, S.; Tracy, J. B.; Frangioni, J. V.; Bawendi, M. G. *J. Am. Chem. Soc.* **2005**, *127*, 10526.
(8) (a) Medintz, I. L.; Clapp, A. R.; Melinger, J. S.; Deschamps, J. R.; Mattoussi, H. *Adv. Mater.* **2005**, *17*, 2450. (b) Medintz, I. L.; Clapp, A. R.; Brunel, F. M.; Tiefenbrunn, T.; Uyeda, H. T.; Chang, E. L.; Deschamps, J. R.; Dawson, P. E.; Mattoussi, H. *Nat. Mater.* **2006**, *5*, 581.
(9) Kotov, N. A.; Dekany, I.; Fendler, J. H. *J. Phys. Chem.* **1995**, *99*, 13065.
(10) Tang, Z. Y.; Zhang, Z. L.; Wang, Y.; Glotzer, S. C.; Kotov, N. A. *Science* **2006**, *314*, 274.
(11) So, M. K.; Xu, C. J.; Loening, A. M.; Gambhir, S. S.; Rao, J. H. *Nat. Biotechnol.* **2006**, *24*, 339.
(12) (a) Gerion, D.; Parak, W. J.; Williams, S. C.; Zanchet, D.; Micheel, C. M.; Alivisatos, A. P. *J. Am. Chem. Soc.* **2002**, *124*, 7070. (b) Gerion, D.; Chen, F. Q.; Kannan, B.; Fu, A. H.; Parak, W. J.; Chen, D. J.; Majumdar, A.; Alivisatos, A. P. *Anal. Chem.* **2003**, *75*, 4766.
(13) (a) Harisinghani, M. G.; Barentsz, J.; Hahn, P. F.; Deserno, W. M.; Tabatabaei, S.; van de Kaa, C. H.; de la Rosette, J.; Weissleder, R. *N. Engl. J. Med.* **2003**, *348*, 2491. (b) Neuwelt, E. A.; Varallyay, P.; Bago, A. G.; Muldoon, L. L.; Nesbit, G.; Nixon, R. *Neuropathol. Appl. Neurobiol.* **2004**, *30*, 456.
(14) (a) Park, J.; An, K. J.; Hwang, Y. S.; Park, J. G.; Noh, H. J.; Kim, J. Y.; Park, J. H.; Hwang, N. M.; Hyeon, T. *Nat. Mater.* **2004**, *3*, 891. (b) Sun, S. H.; Zeng, H. *J. Am. Chem. Soc.* **2002**, *124*, 8204. (c) Chen, M.; Nikles, D. E. *J. Appl. Phys.* **2002**, *91*, 8477. (d) Kang, S.; Harrell, J. W.; Nikles, D. E. *Nano Lett.* **2002**, *2*, 1033. (e) Tzitzios, V.; Niarchos, D.; Gjoka, M.; Boukos, N.; Petridis, D. *J. Am. Chem. Soc.* **2005**, *127*, 13756. (f) Peng, S.; Sun, S. H. *Angew. Chem., Int. Ed.* **2007**, *46*, 4155. (g) Kim, D.; Park, J.; An, K.; Yang, N. K.; Park, J. G.; Hyeon, T. *J. Am. Chem. Soc.* **2007**, *129*, 5812. (h) Chen, M.; Pica, T.; Jiang, Y. B.; Li, P.; Yano, K.; Liu, J. P.; Datye, A. K.; Fan, H. Y. *J. Am. Chem. Soc.* **2007**, *129*, 6348. (i) Kovalenko, M. V.; Bodnarchuk, M. I.; Lechner, R. T.; Hesser, G.; Schaffler, F.; Heiss, W. *J. Am. Chem. Soc.* **2007**, *129*, 6352.
(15) Sun, S. H.; Murray, C. B.; Weller, D.; Folks, L.; Moser, A. *Science* **2000**, *287*, 1989.
(16) (a) Gu, H. W.; Ho, P. L.; Tsang, K. W. T.; Wang, L.; Xu, B. *J. Am. Chem. Soc.* **2003**, *125*, 15702. (b) Gu, H. W.; Ho, P. L.; Tsang, K. W. T.; Yu, C. W.; Xu, B. *Chem. Commun.* **2003**, 1966. (c) Lee, H.; Lee, E.; Kim, D. K.; Jang, N. K.; Jeong, Y. Y.; Jon, S. *J. Am. Chem. Soc.* **2006**, *128*, 7383. (d) Xu, C. J.; Xu, K. M.; Gu, H. W.; Zheng, R. K.; Liu, H.; Zhang, X. X.; Guo, Z. H.; Xu, B. *J. Am. Chem. Soc.* **2004**, *126*, 9938. (e) Xu, C. J.; Xu, K. M.; Gu, H. W.; Zhong, X. F.; Guo, Z. H.; Zheng, R. K.; Zhang, X. X.; Xu, B. *J. Am. Chem. Soc.* **2004**, *126*, 3392. (f) Gu, H. W.; Xu, K. M.; Xu, C. J.; Xu, B. *Chem. Commun.* **2006**, 941. (g) Lee, I. S.; Lee, N.; Park, J.; Kim, B. H.; Yi, Y. W.; Kim, T.; Kim, T. K.; Lee, I. H.; Paik, S. R.; Hyeon, T. *J. Am. Chem. Soc.* **2006**, *128*, 10658. (h) Jun, Y. W.; Huh, Y. M.; Choi, J. S.; Lee, J. H.; Song, H. T.; Kim, S.; Yoon, S.; Kim, K. S.; Shin, J. S.; Suh, J. S.; Cheon, J. *J. Am. Chem. Soc.* **2005**, *127*, 5732. (i) Wang, L.; Yang, Z. M.; Gao, J. H.; Xu, K. M.; Gu, H. W.; Zhang, B.; Zhang, X. X.; Xu, B. *J. Am. Chem. Soc.* **2006**, *128*, 13358. (j) Sun, S. H. *Adv. Mater.* **2006**, *18*, 393. (k) Gao, J. H.; Li, L. H.; Ho, P. L.; Mak, G. C.; Gu, H. W.; Xu, B. *Adv. Mater.* **2006**, *18*, 3145.
(17) (a) Josephson, L.; Tung, C. H.; Moore, A.; Weissleder, R. *Bioconjugate Chem.* **1999**, *10*, 186. (b) Lewin, M.; Carlesso, N.; Tung, C. H.; Tang, X. W.; Cory, D.; Scadden, D. T.; Weissleder, R. *Nat. Biotechnol.* **2000**, *18*, 410.
(18) Kircher, M. F.; Allport, J. R.; Graves, E. E.; Love, V.; Josephson, L.; Lichtman, A. H.; Weissleder, R. *Cancer Res.* **2003**, *63*, 6838.
(19) Gu, H. W.; Zheng, R. K.; Zhang, X. X.; Xu, B. *J. Am. Chem. Soc.* **2004**, *126*, 5664.
(20) Kwon, K. W.; Shim, M. *J. Am. Chem. Soc.* **2005**, *127*, 10269.
(21) Gu, H. W.; Zheng, R. K.; Liu, H.; Zhang, X. X.; Xu, B. *Small* **2005**, *1*, 402.
(22) Wang, D. S.; He, J. B.; Rosenzweig, N.; Rosenzweig, Z. *Nano Lett.* **2004**, *4*, 409.
(23) Kim, H.; Achermann, M.; Balet, L. P.; Hollingsworth, J. A.; Klimov, V. I. *J. Am. Chem. Soc.* **2005**, *127*, 544.
(24) Pellegrino, T.; Fiore, A.; Carlino, E.; Giannini, C.; Cozzoli, P. D.; Ciccarella, G.; Respaud, M.; Palmirotta, L.; Cingolani, R.; Manna, L. *J. Am. Chem. Soc.* **2006**, *128*, 6690.
(25) Yu, H.; Chen, M.; Rice, P. M.; Wang, S. X.; White, R. L.; Sun, S. H. *Nano Lett.* **2005**, *5*, 379.
(26) Mokari, T.; Sztrum, C. G.; Salant, A.; Rabani, E.; Banin, U. *Nat. Mater.* **2005**, *4*, 855.
(27) Gu, H. W.; Yang, Z. M.; Gao, J. H.; Chang, C. K.; Xu, B. *J. Am. Chem. Soc.* **2005**, *127*, 34.
(28) (a) Perro, A.; Reculusa, S.; Ravaine, S.; Bourgeat-Lami, E. B.; Duguet, E. *J. Mater. Chem.* **2005**, *15*, 3745. (b) Shi, W. L.; Zeng, H.; Sahoo, Y.; Ohulchanskyy, T. Y.; Ding, Y.; Wang, Z. L.; Swihart, M.; Prasad, P. N. *Nano Lett.* **2006**, *6*, 875.

Scheme 1. Some Reagent Addition Sequences and the Corresponding Products

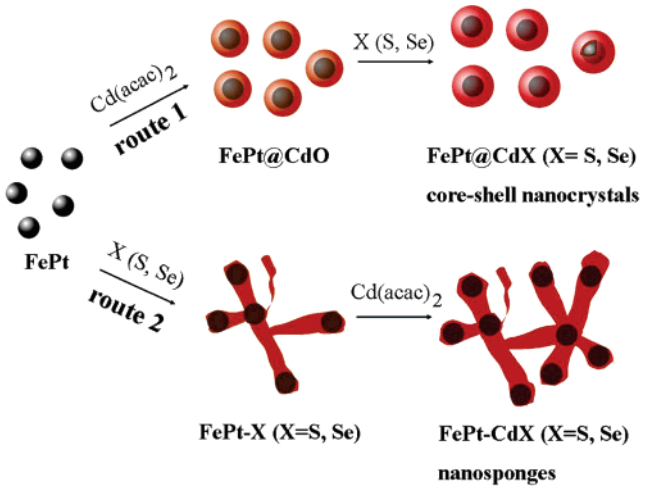

first reported nanostructures with a FePt magnetic core and a CdX shell. Their combination of superparamagnetism and fluorescence at nanometer scale should help expand the biological applications of multifunctional nanomaterials. They might, for example, serve as bimodal imaging probes for MRI and fluorescence microscopy,[29] in which case they may represent a new class of agents for molecular imaging.

2. Experimental Section

2.1. Chemicals. Oleic acid (99%), oleylamine (99%), sulfur precipitate (99.998%), selenium powder (99.5%), tellurium powder (99.9%), trioctylphosphine oxide (TOPO; technical grade, 90%), hexadecane-1,2-diol (technical grade, 90%), phenyl ether (99%), dioctyl ether (99%), benzyl ether (99%), and 1,2-dichlorobenzene were purchased from Sigma-Aldrich Corp. and $Fe(CO)_5$, $Pt(acac)_2$ (98%), and $Cd(acac)_2$ (99%) from Strem Chemicals Inc. All the chemical reactions were carried out under an inert atmosphere in a glovebox to prevent oxidation unless otherwise stated.

2.2. Typical Synthesis of FePt@CdSe Core−Shell Nanocrystals. After the method reported by Sun et al.[15] was used to form FePt nanoparticles via the thermolysis of $Fe(CO)_5$ (0.07 mL) and $Pt(acac)_2$ (50 mg) in phenyl ether, the solution (about 15 mL) was cooled to 200 °C. Without further separation or purification, $Cd(acac)_2$ (312 mg) and hexadecane-1,2-diol (500 mg) were added, and the mixture was held at 200 °C for 30 min to decompose the $Cd(acac)_2$ precursor to form FePt@CdO core−shell intermediate nanostructures. The solution changed from black to dark brown, indicating the formation of CdO after the thermal decomposition of $Cd(acac)_2$, similar to the decomposition of $Zn(acac)_2$.[30] Selenium powder (85 mg) was then added, and the reaction mixture was heated to refluxing (258 °C) for 60 min, which resulted in a black dispersion of FePt@CdSe core−shell nanocrystals. The reaction mixture was allowed to cool to room temperature after removal of the heat source. Ethanol (20 mL) was added to the mixture, and the black product was precipitated via centrifugation. Washing the product with ethanol and hexane can easily purify the core−shell nanocrystals thus produced. The final product redispersed well in hexane.

2.3. Typical Synthesis of FePt−CdS Nanosponges. After formation of FePt nanoparticles by thermal decomposition of $Fe(CO)_5$ (0.07 mL) and $Pt(acac)_2$ (50 mg) in phenyl ether, the solution was cooled to 120 °C. Without any separation or purification, sulfur precipitate (35 mg) was added, and the temperature was held at 120 °C for 10 min, $Cd(acac)_2$ (312 mg) was then added, and the temperature was raised to 200 °C at the rate of 10 °C/min and then maintained for 10 min. In the final step, the hot solution (15 mL) was heated quickly to refluxing (about 258 °C) and left to reflux for 45 min to give a black dispersion of FePt−CdS nanosponges. The product purification procedure was similar to that described above.

2.4. Synthesis of FePt−CdSe Heterodimers of Nanocrystals. After formation of FePt nanoparticles by thermal decomposition of $Fe(CO)_5$ (0.07 mL) and $Pt(acac)_2$ (50 mg) in benzyl ether (or dioctyl ether), the solution was cooled to 200 °C. Without any separation or purification, $Cd(acac)_2$ (312 mg) was added, and the temperature was maintained at 200 °C for 30 min. Selenium powder (85 mg) was then added, and the mixture was heated to refluxing (about 300 °C in benzyl ether, about 286 °C in dioctyl ether) and held there for 90 min to give a black dispersion of FePt−CdSe heterodimers of the nanocrystals.

2.5. Instrumentation. Transmission electron micrographs were obtained using a JEOL 2010 electron microscope operated at 200 kV. High-resolution transmission electron microscopy (HRTEM) images and energy-dispersive X-ray (EDX) microanalysis were obtained with this equipment. Absorbance and fluorescence spectra were recorded on a Perkin-Elmer Lambda 900 UV/vis/NIR spectrometer and a Perkin-Elmer luminescence spectrometer (LS55), respectively, and fluorescence micrographs were recorded with an Olympus BX41 microscope.

3. Results

3.1. Formation of FePt@CdX (X = S, Se) Core−Shell Nanocrystals. The thermolysis of $Pt(acac)_2$ and $Fe(CO)_5$ according to the procedure reported by Sun and co-workers[15] yielded monodispersed FePt nanoparticles with a diameter of approximately 3 nm (Figure 1A). Selected-area electron diffraction (SAED) indicated that these FePt nanoparticles were in a disordered face-centered cubic (fcc) phase (Figure 1A, inset). After the addition of cadmium sources, $Cd(acac)_2$, and reaction at 200 °C for about 30 min, the subsequent addition of chalcogens afforded FePt@CdX (X = S or Se) core−shell nanocrystals (route 1 in Scheme 1). TEM images clearly display the monodispersed core−shell nanocrystal structure. While the FePt@CdS nanocrystals (Figure 1B) showed some degree of aggregation and fusion of the nanocrystals, the FePt@CdSe core−shell nanocrystals (Figure 1C) exhibited much better monodispersity (around 10 nm outside diameter with a 3 nm diameter of the FePt core). HRTEM images (Figure 1B,C, insets) suggest that both the FePt parts and the CdS or CdSe parts were crystalline. EDX spectrometry of FePt@CdS core−shell nanocrystals (Supporting Information, Figure S1) showed that the core consisted primarily of Fe and Pt and the shell of Cd and S, corresponding to regions 1 and 2, respectively, in the figure (the signals of Fe and Pt in region 2 should originate from FePt cores). EDX spectrometry of the FePt@CdSe core−shell nanocrystals (Figure S1) also confirmed that the cores consisted primarily of Fe and Pt and the shells of Cd and Se, corresponding to regions 3 and 4, respectively.

Both kinds of core−shell nanocrystals described above should exhibit both fluorescence and superparamagnetism. The UV/vis absorption peak at ~435 nm shown in Figure 2A corresponds to CdS in the FePt@CdS core−shell nanocrystals, though it is a weak peak. The fluorescence spectrum indicates a fluorescence maximum for FePt@CdS nanocrystals at ~460 nm, which is similar to that of about 5 nm sized CdS nanoparticles.[31] The FePt@CdSe core−shell nanocrystals exhibited an absorption peak at ~445 nm (Figure 2B) resulting from the CdSe shells.

(29) Mulder, W. J. M.; Koole, R.; Brandwijk, R. J.; Storm, G.; Chin, P. T. K.; Strijkers, G. J.; Donega, C. D.; Nicolay, K.; Griffioen, A. W. *Nano Lett.* **2006**, *6*, 1.
(30) Hussien, G. A. M. *Thermochim. Acta* **1991**, *186*, 187.

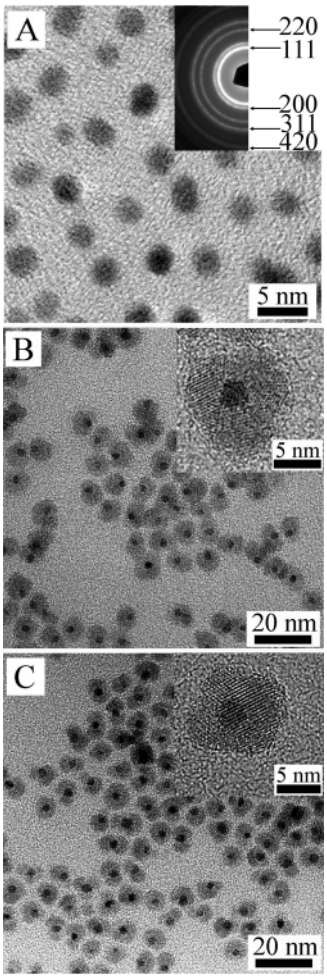

Figure 1. TEM images of (A) as-prepared FePt nanoparticles (inset: SAED pattern analysis of FePt), (B) FePt@CdS core−shell nanocrystals (inset: HRTEM image), and (C) FePt@CdSe core−shell nanocrystals (inset: HRTEM image).

Interestingly, the fluorescence spectrum of the FePt@CdSe nanocrystals showed a fluorescence emission peak at ∼465 nm, which is similar to that reported for 2 nm CdSe nanoparticles.[32] The fluorescence emission peaks in Figure 2A,B are slightly asymmetric, which can be explained by variation in the crystallinity of the CdS (or CdSe) shells around the FePt cores. Compared with the symmetric photoluminescence (PL) peaks of neat CdS (or CdSe) nanocrystals,[33] the asymmetric PL peaks of these two samples suggest the fluorescent properties originated from the FePt@CdS core−shell nanoparticles (or FePt@CdSe core−shell nanoparticles). Moreover, the emission peaks are broad (the full width at half-maximum (fwhm) is about 50−70 nm), which is likely due to the presence of multicrystalline CdS (or CdSe) shells (see the HRTEM images in Figure 1). There may perhaps be many CdS (or CdSe) clusters with different sizes and shapes in the multicrystalline CdS (or CdSe) shells. Since the emission peak of a semiconducting nanoparticle is strongly dependent on its size and shape,[33] the CdS (or CdSe) nanoclusters' crystallite domains[23] with different sizes and shapes result in the broad emission spectra. The blue emission color (about 465 nm) of the FePt@CdSe core−shell nanocrystals may result from the small size (about 2 nm in diameter[32]) of the CdSe nanoclusters in shells around the FePt cores. Upon illumination of a hand-held UV lamp (λ_{ex} = 365 nm), the FePt@CdX (X = S or Se) core−shell nanocrystal dispersion gives off blue emissions (Figure 2C,D), which is consistent with the emission peaks in the fluorescence spectra. At room temperature, the fluorescence quantum yield (QY) of FePt@CdS core−shell nanocrystals is 2.3−3.5%, while that of FePt@CdSe core−shell nanocrystals is a little higher at 7.5−9.7%.[34] The relatively low QYs of such multifunctional nanocrystals can be a result of the partial quenching due to metallic (FePt) cores, similar to the case of the Co@CdSe core−shell nanostructures reported by Klimov et al.[23] The photoluminescence excitation (PLE) spectra (Figure S2, Supporting Information) of FePt@CdS core−shell and FePt@CdSe core−shell nanoparticles are similar in shape to the corresponding UV/vis spectra, indicating the fluorescent properties of the nanoparticles are independent of the excitation wavelength.

Magnetic measurements were performed immediately after the synthesis of the core−shell nanocrystals. Standard zero-field cooling (ZFC) and field cooling (FC) measurements gave estimated blocking temperatures of about 13 K for the FePt@CdS core−shell nanocrystals and 14 K for the FePt@CdSe core−shell nanocrystals (Figure 3), suggesting that the superparamagnetic behavior of the FePt core essentially was preserved. That is, the CdX shell had little effect on the magnetic properties of the core. The well-defined sharp peaks indicate the uniform size of the FePt cores and rather weak magnetic dipolar interactions between the FePt parts in these two samples. This is confirmed by extrapolating the plots of $1/m$ against T to pass through the origins (Figure 3, insets), showing that nanostructures with CdX (X = S or Se) shells should minimize the interactions between the FePt cores.

To test the stability of these types of nanoparticles in potential biological applications, we chose FePt@CdSe core−shell nanoparticles as an example for the surface modification. After being modified by glutathione (GSH) molecules, the nanoparticles dispersed in water very well and also maintained the core−shell nanostructures (Figure S3, Supporting Information), indicating these types of nanoparticles were robust enough to meet the essential requirements in biological applications.

3.2. Formation of FePt−CdX (X = S, Se) Nanosponges. Route 2 in Scheme 1 afforded only spongelike nanonetworks (Figure 4A,B). The FePt nanoparticles apparently served as a center from which CdX (X = S or Se) nanowires could branch out, and all the FePt nanoparticles were coated with different amounts of CdX (X = S or Se). HRTEM images (insets in Figure 4A,B) indicate that the FePt parts and the CdX (X = S or Se) parts were all crystalline. The FePt−CdX nanosponges also exhibited fluorescence. Because of their low solubility, UV/vis and fluorescence spectra were recorded with solid-state samples (Figure S4, Supporting Information). UV/vis absorption peaks of these two nanosponges appeared at ∼510 nm. The fluorescence emission peaks of these two nanosponge samples appeared at ∼530 nm with a Stokes shift of about 20 nm. To

(31) (a) Joo, J.; Na, H. B.; Yu, T.; Yu, J. H.; Kim, Y. W.; Wu, F. X.; Zhang, J. Z.; Hyeon, T. *J. Am. Chem. Soc.* **2003**, *125*, 11100. (b) Steckel, J. S.; Zimmer, J. P.; Coe-Sullivan, S.; Stott, N. E.; Bulovic, V.; Bawendi, M. G. *Angew. Chem., Int. Ed.* **2004**, *43*, 2154.

(32) Murray, C. B.; Norris, D. J.; Bawendi, M. G. *J. Am. Chem. Soc.* **1993**, *115*, 8706.

(33) (a) Peng, X. G.; Manna, L.; Yang, W. D.; Wickham, J.; Scher, E.; Kadavanich, A.; Alivisatos, A. P. *Nature* **2000**, *404*, 59. (b) Qu, L. H.; Peng, X. G. *J. Am. Chem. Soc.* **2002**, *124*, 2049. (c) Peng, Z. A.; Peng, X. G. *J. Am. Chem. Soc.* **2002**, *124*, 3343.

(34) See the Supporting Information.

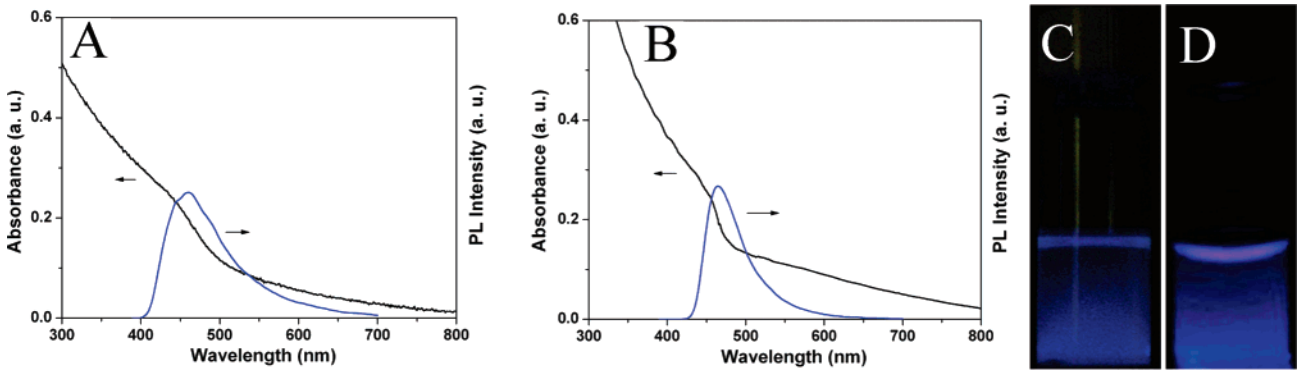

Figure 2. UV/vis and fluorescence spectra (λ_{ex} = 365 nm) of (A) FePt@CdS core−shell nanocrystals and (B) FePt@CdSe core−shell nanocrystals in a hexane suspension. Fluorescence images of hexane solutions of (C) FePt@CdS core−shell nanocrystals and (D) FePt@CdSe core−shell nanocrystals excited by a UV lamp (λ_{ex} = 365 nm).

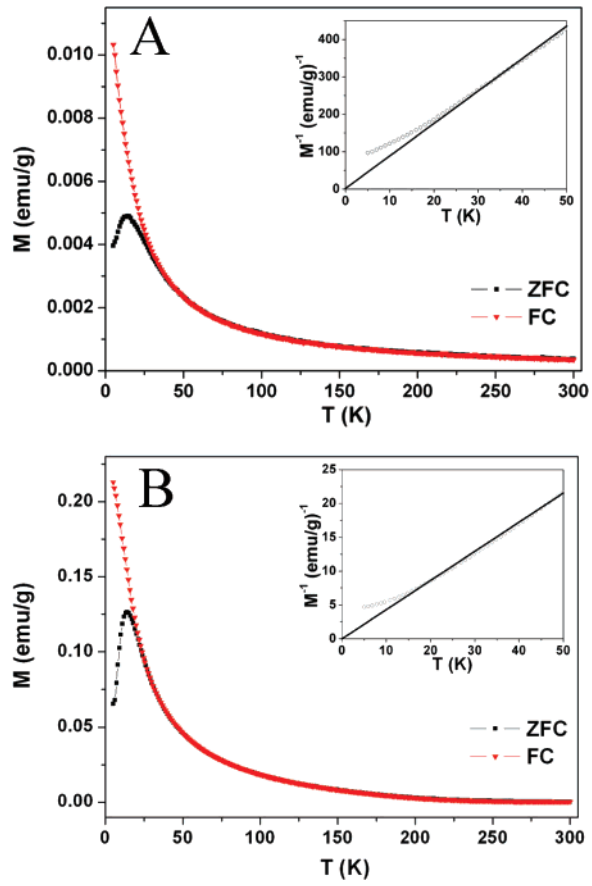

Figure 3. Temperature dependence of the ZFC/FC magnetization of (A) FePt@CdS core−shell nanocrystals and (B) FePt@CdSe core−shell nanocrystals with a magnetic field of 100 Oe (insets: FC, 1/*m* vs *T*).

observe the fluorescence of the samples directly, fluorescent images (excitation range 460−490 nm) were taken under a microscope. FePt−CdS nanosponges and FePt−CdSe nanosponges both displayed green emissions (Figure 4C,D), which were consistent with the emission peaks in the fluorescence spectra (Figure S4). ZFC/FC measurements gave estimated blocking temperatures of 9 K for the FePt−CdS nanosponges and 14 K for the FePt−CdSe nanosponges (Figure 4E,F), indicating that they were superparamagnetic at room temperature. The blocking temperature of the FePt−CdS nanosponges was lower than that of the FePt−CdSe nanosponges because of the smaller size of the FePt nanoparticles (about 2 nm) in FePt−CdS nanosponges. The divergence of the ZFC and FC curves at temperatures higher than the blocking temperature could be due to the relatively broad size distribution of the FePt nanoparticles and relatively strong magnetic interactions between particles, suggesting that some of the FePt nanoparticles were close to each other in the nanosponges (Figure 4A,B).

3.3. Formation of FePt−CdSe Heterodimer Nanocrystals. When much higher boiling point solvents such as benzyl ether (boiling point 300 °C) or dioctyl ether (boiling point 286 °C) replaced phenyl ether (boiling point 258 °C) in the FePt@CdSe core−shell nanocrystal synthesis, only FePt−CdSe heterodimer nanocrystals were formed, as shown in Figure 5. The diameters of the FePt particles remained at ∼3 nm, but the CdSe component had diameters of 6−8 nm (Figure 5A). An HRTEM image shows that the CdSe parts were crystalline (Figure 5B). The FePt−CdSe heterodimer nanocrystals retained the properties of their individual components (FePt and CdSe), like the FePt−CdS heterodimer nanoparticles that have previously been reported.[19] As shown in Figure 5C,D, the FePt−CdSe heterodimer nanocrystals exhibited fluorescence emission maxima at ∼460 nm (UV/vis absorption peak at ∼437 nm) and had an estimated blocking temperature of ∼10 K according to standard ZFC/FC measurements.

4. Discussion

4.1. Effect of the Precursor Addition Sequence. The sequence of addition of the reagents played a determining major role in the formation of these multifunctional nanostructures. To further demonstrate the formation mechanism proposed in Scheme 1, stepwise characterization experiments were performed. After the addition of cadmium precursors, FePt@CdO core−shell intermediate nanostructures (Figure S5, Supporting Information) formed easily, probably because FePt (a = 3.816 Å) and CdO (a = 4.695 Å) have the same face-centered cubic lattice structures (space group $Fm3m$). Thus, FePt@CdX (X = S or Se) core−shell nanocrystals result after the addition of the corresponding chalcogen (Figure 1B,C).

It is also known that chalcogens such as selenium and tellurium easily form nanowires in a high-temperature solvent when surfactants are present. Similar to the results reported by Xia et al.,[35] selenium nanowires were also observed to form readily in these experiments upon the addition of selenium powder to a hot 1,2-dichlorobenzene solution containing TOPO

(35) (a) Gates, B.; Mayers, B.; Cattle, B.; Xia, Y. N. *Adv. Funct. Mater.* **2002**, *12*, 219. (b) Xia, Y. N.; Yang, P. D.; Sun, Y. G.; Wu, Y. Y.; Mayers, B.; Gates, B.; Yin, Y. D.; Kim, F.; Yan, Y. Q. *Adv. Mater.* **2003**, *15*, 353.

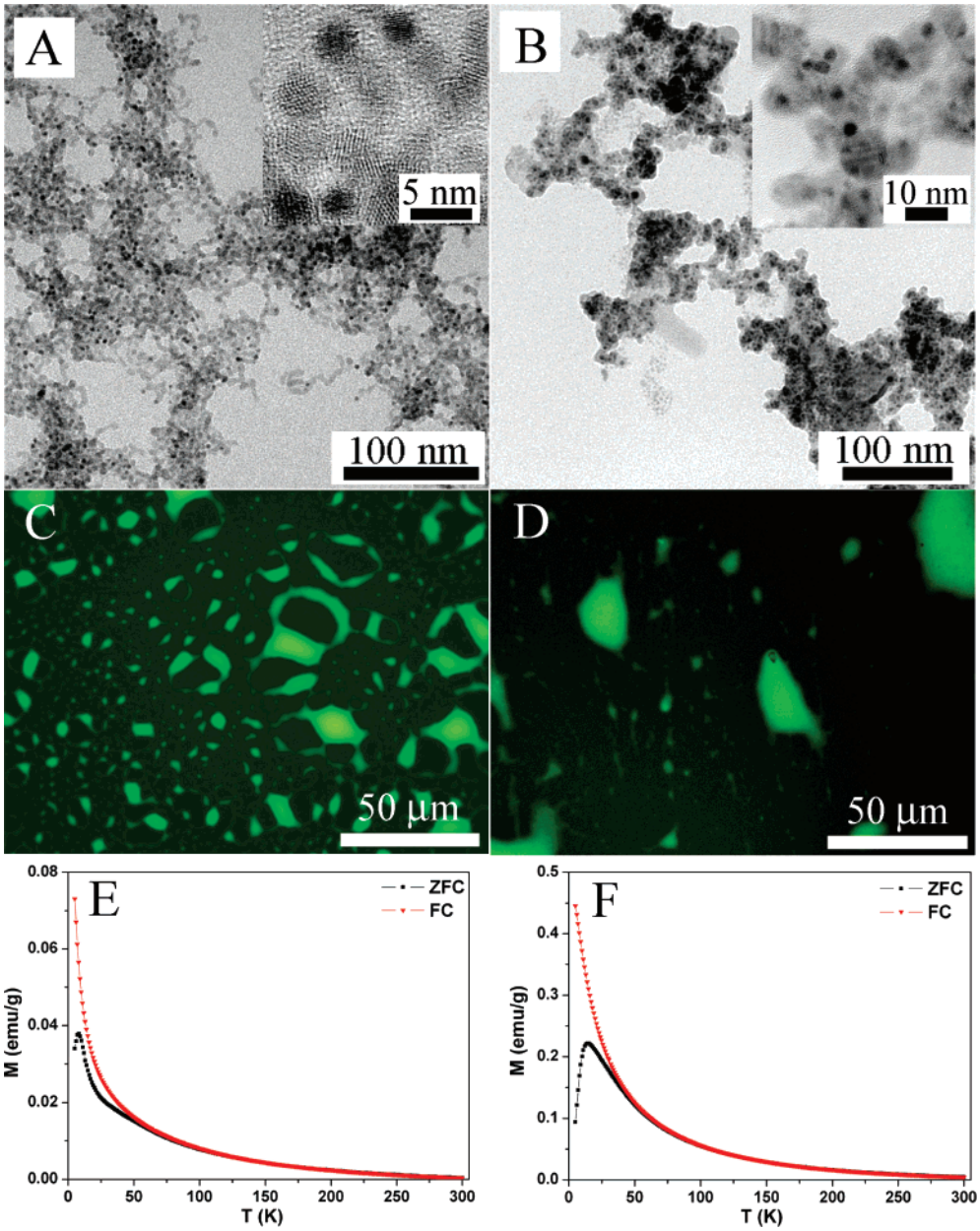

Figure 4. TEM images of (A) FePt−CdS nanosponges and (B) FePt−CdSe nanosponges (insets: HRTEM images). Fluorescence microscope images of aggregations of (C) FePt−CdS nanosponges and (D) FePt−CdSe nanosponges. The nanosponges were spread on a glass slide and the images taken with a fluorescence microscope (excitation wavelength range 460−490 nm). Temperature dependence of the ZFC/FC magnetizations of (E) FePt−CdS nanosponges and (F) FePt−CdSe nanosponges with a magnetic field of 100 Oe.

surfactant (Figure S6, Supporting Information). The resulting Se nanowires were 10−80 nm in width and crystalline. As shown in route 2 (Scheme 1), when the chalcogen precursors were added to the hot organic suspension containing FePt nanoparticles, the chalcogen nanowires with FePt nanoparticles as nodes formed immediately (Figure S7, Supporting Information), and the subsequence addition of a cadmium source yielded the corresponding FePt−CdX nanosponge network (Figure 4A,B).

4.2. Role of Temperature. High-boiling-point organic solvents are frequently used to synthesize nanostructures through the thermolysis of precursors. For the synthesis of core−shell nanocrystals and nanosponges, phenyl ether with a boiling point of 258 °C was chosen as the reaction solvent. Had a solvent with much higher boiling point been chosen, the nanostructure of the products would have been different. FePt−CdS heterodimers are produced with dioctyl ether (boiling point 286 °C) as the reaction solvent.[19] With benzyl ether (boiling point 300 °C), reactions following route 1 (Scheme 1) yielded FePt−CdX (X = S or Se) heterodimer nanocrystals as the only product. The formation of nanocrystals at the higher temperature is probably due to the difference in phase transition temperatures between the FePt and CdX (X = S or Se) components.[19] The CdX (X = S or Se) component may melt at the higher temperature and induce dewetting from the FePt cores, resulting in the formation of heterodimeric nanocrystals.

4.3. Reaction Time. To investigate the formation process and the thermal stability of the FePt@CdSe core−shell nanocrystals, the course of their synthesis reaction in phenyl ether was tracked at 30 min intervals. As shown in Figure 6, 30 min

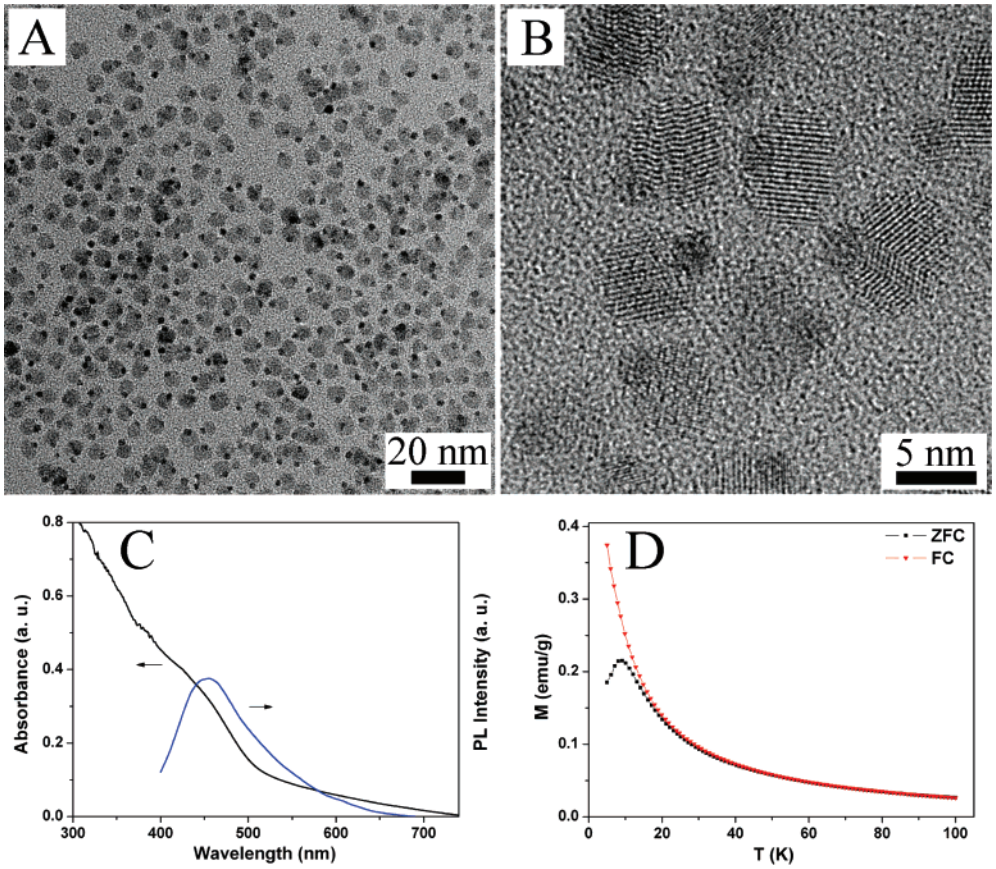

Figure 5. (A) TEM image and (B) HRTEM image of FePt−CdSe heterodimer nanocrystals formed over 90 min at about 300 °C using benzyl ether as the reaction solvent. (C) UV/vis and fluorescence spectra (λ_{ex} = 365 nm) of FePt−CdSe heterodimer nanocrystals in hexane. (D) Temperature-dependent magnetization (ZFC/FC) of FePt−CdSe heterodimer nanocrystals measured with a magnetic field of 100 Oe.

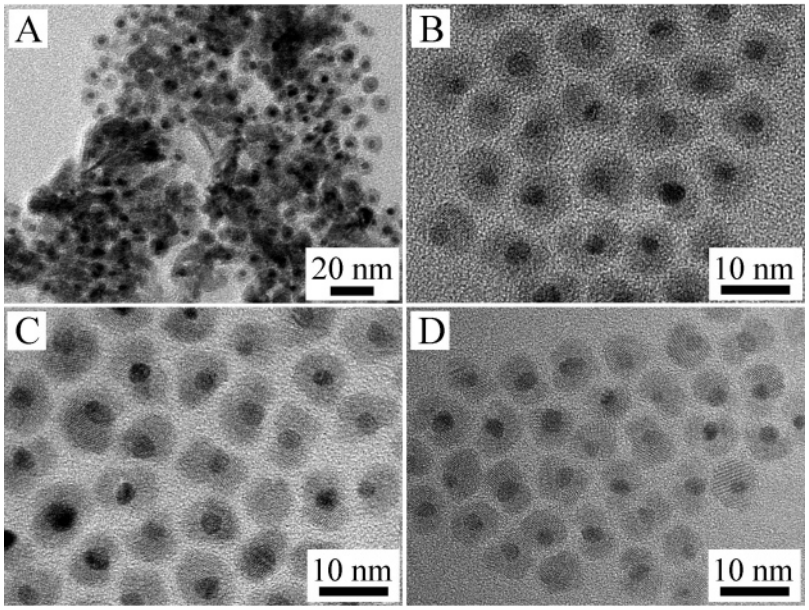

Figure 6. TEM images of FePt@CdSe core−shell nanocrystals formed in reactions lasting (A) 30 min, (B) 60 min, (C) 90 min, and (D) 120 min.

after the addition of Se stock solution, some FePt@CdSe core−shell nanocrystals about 10 nm in diameter had been produced (Figure 6A), in addition to amorphous material. This amorphous material may have been precursors which had not yet reacted, suggesting that the reaction was incomplete after 30 min. The reaction was finished completely after 60 min, yielding FePt@CdSe core−shell nanocrystals of uniform size (Figure 6B). When the reaction time was lengthened to 90 or even 120 min, the nanocrystals still maintained their core−shell nanostructure without any further evolution (Figure 6C,D), indicating that FePt@CdSe core−shell nanocrystals are stable in hot solution during prolonged refluxing.

Table 1. Products Formed under Different Conditions

	sequence of addn				
	first addn	second addn	solvent (boiling point, °C)	reaction time (min)	final products
1	$Cd(acac)_2$	S	phenyl ether (258)	60−70	core−shell nanocrystals
	$Cd(acac)_2$	Se	phenyl ether (258)	60−70	core−shell nanocrystals
2	S	$Cd(acac)_2$	phenyl ether (258)	45−60	nanosponges
	Se	$Cd(acac)_2$	phenyl ether (258)	50−60	nanosponges
3	$Cd(acac)_2$	S	dioctyl ether (286)	80−90	heterodimer nanocrystals[19]
		Se	benzyl ether (300) or dioctyl ether (286)	80−90	heterodimer nanocrystals

5. Conclusion

These experiments have shown that the one-pot synthetic procedure for FePt nanoparticles and semiconducting chalcogenides can be fine-tuned to generate core−shell nanocrystals or nanosponges. Altering the sequence of addition of the reagents is the most effective factor (Table 1). The synthesis of these core−shell nanocrystals, nanosponges, or heterodimer nanocrystals is highly reproducible and general. The same synthesis can be extended to yield FePt@CdTe core−shell nanocrystals (Figure S8, Supporting Information). Although the optical properties of these nanostructures must still be improved for higher quantum yields (replacing the metallic core with an oxide core such as iron oxide, perhaps), this rather simple approach indeed opens an avenue to sophisticated and multifunctional nanostructures that promise new applications in microelectronics, biology, and medicine.

Acknowledgment. This work was partially supported by RGC, HIA (HKUST), and E. I. du Pont de Nemours and Co.

Supporting Information Available: Detailed Experimental Section, quantum yields, and Figures S1−S8. This material is available free of charge via the Internet at http://pubs.acs.org.

JA0731017